

Extraction and characterization of novel natural lignocellulosic fibers from *Malva sylvestris* L.

Journal of Composite Materials
2023, Vol. 57(5) 897–912
© The Author(s) 2022
Article reuse guidelines:
sagepub.com/journals-permissions
DOI: 10.1177/00219983221146355
journals.sagepub.com/home/jcm


Mostefa Meddah, Mansour Rokbi and Moussa Zaoui

Abstract

The main goal of this study is to characterize natural lignocellulosic fibers extracted from *Malva Sylvestris*. The experimental approach used is consisted to analyze the morphological, physical, chemical, thermal and mechanical characteristics of *Malva sylvestris* fibers. The stem anatomy showed that the bark of *Malva* is rich in fiber cells. Based on ATR-FTIR and X-ray analysis, the obtained results illustrated that the fiber contained mainly cellulose, hemicellulose and lignin. The crystallinity index of fiber is about 55.12 %, which indicated a high cellulose content. The Thermo-gravimetric analysis (TGA) analysis test point out that *Malva Sylvestris* fibers are thermally stable until 225°C and an apparent activation energy about of 111 kJ.mol⁻¹ was recorded. Tensile strength of *Malva* fibers is about of 236.64 ± 93.33 MPa whilst its young's modulus is about of 26.07 ± 5.14 GPa. In view of the dispersion in the obtained experimental results, the latter were analyzed using the Weibull statistical laws with two parameters.

Keywords

Malva sylvestris L, lignocellulosic, stem anatomy, ATR-FTIR, X-ray, thermo-gravimetric analysis, mechanical properties

Introduction

During the last 30 years, the reinforcement of composite materials with synthetic fibers has generated considerable interest for retrofitting existing structures.¹ Although the incorporation of this kind of fibers in the composite materials can make improvements to its composites (high strength to weight ratios, higher fatigue strength, better resistance to corrosion and acids). In contrast, the use of synthetic fibers as reinforcement agent in composites can be accompanied by several disadvantages such as high cost, high density, poor recycling, non-biodegradable, non-environmentally.² That is why in the recent years, an apparent awareness of environmental issues has developed. This consciousness arises through the serious ecological, and health hazard problems. Consequently, progressive technological demands and environmental legislation have raised increasing interest in renewable, biodegradable and natural materials.³

During the last two decades, more sustainable natural fibers reinforced resin matrix composites are being used for environmental needs as alternatives for synthetic ones.^{4,5} Although there are some limitations of natural fiber compared to human-made fiber, such as, the variation in fiber performances, low thermal stability, weak bonding between

fiber-matrix,⁶ considerable effort has been devoted to the development of new environmentally friendly and low-cost material composites by replacing synthetic fibers such as glass, aramid, nylon and carbon fibers by lignocellulosic ones.^{4,7,8} Despite its advantages, synthetic fibers have recently become undesirable because of the difficulty of eliminating these products after their life end.⁹ Conversely, lignocellulosic fibers are easily biodegradable with a limited environmental impact. Added to this, many advantages, such as their distinct mechanical properties (high specific strength, light weight, qualitative coefficients and flexibility), reduce skin irritation, abundant material and inexpensive treatment, can justified the use of cellulosic fibers as reinforcing elements for composite materials and/or textile industry.¹⁰ Indeed, an exponential growth in publications of research papers and reviews of “natural fiber composites” has been observed over the past 20 years (Figure 1), This can be explained by the increasing demand of bio-

Department of Mechanical Engineering, University of M'sila, Algeria

Corresponding author:

Mansour Rokbi, Department of Mechanical Engineering, University of M'sila, University pole of M'sila, Algeria.
Email: mansour.rokbi@univ-msila.dz

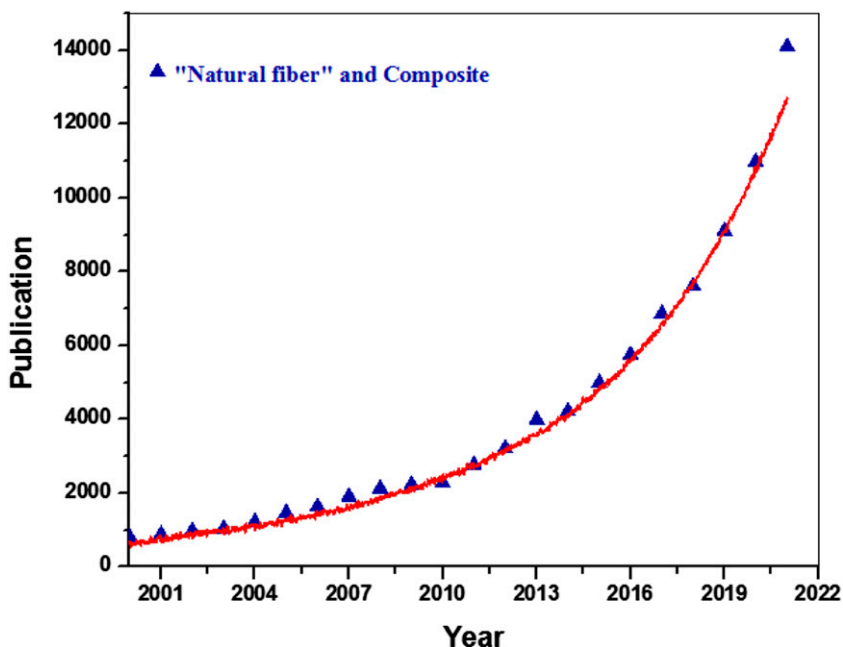


Figure 1. Publication by year for “Natural fiber and composite” according to science direct database.

composite, also named green composites, as alternative materials to substitute synthetic fibers. It is in this context that this investigation was conducted to provide long lignocellulosic fibers. These last are characterized by suitable properties for polymeric composite materials and textile applications.¹⁰ The degradation pathway of cellulose is typically driven through hydrolysis mediated by the family of cellulose enzymes. Moreover, besides being recyclable and degradable, they provide a wide range of exciting properties, including excellent mechanical, barrier, and thermal properties.^{11–13}

There are many types of plants that have attracted researchers and industrialists for this purpose. Depending on its origin, cellulosic fibers can be extracted from different sources; stem, leaf, petioles, roots, fruits and seeds. The characteristics of natural fibers are strongly influenced by (i) the maturity of the plant, (ii) climatic conditions of weather circumstances, and (iii) extraction process.^{14–16} The chemical structure of natural fiber consisting of polysaccharides polymer (i.e cellulose and hemicelluloses) and the aromatic polymer (i.e lignin) as well as by some non-structural components (i.e. proteins, extractives).^{17,18}

The remarkable characteristics of natural fibers have made them an important axis of scientific research and industrial use in composite materials. These fibers are widely used in many applications such as automobile parts, electrical, marine, sports and aerospace. For all this, much research has been conducted on new cellulosic fibers to test their ability as reinforcement of polymeric matrices. Therefore, a very large amount of research on the characterization of new fibers has been established. These new

fibers were extracted from the leaf,^{14,15} the stem,^{19–21} the bark,^{22–24} the fruits^{25,26} or from the roots of a plant.^{27–29} To our knowledge, there is unfortunately no study yet on the characterization of physical, chemical and mechanical properties of *Malva sylvestris* fibers. On the other, there are three reasons that support the study of *Malva sylvestris* L. plant: the abundance, the easy extraction and the structure of the obtained fiber (long fiber). First all, *Malva sylvestris* L. plant is abundant in north Africa and specifically in Algeria, and can be harvested with very simple means. Secondly, *Malva sylvestris* L. fiber can be easily extracted from the stem using an eco-friendly technique. And the extraction was done within a short time. Thirdly, by using a water retting extraction process, longer length fibers can be extracted from the stems of *Malva sylvestris* L. plant. As indicated in literature, long fibers can provide exceptional opportunities to develop a new class of advanced lightweight composites,³⁰ and have the potential to rival glass fiber in the manufacture of composite materials.³¹ In this study, a comprehensive morphological, physical, chemical and mechanical properties of *Malva sylvestris* fibers were investigated as promising alternative to replace synthetic fibers to use as reinforcement element for polymer matrix.

Materials and experimental procedure

Raw material

Malva sylvestris L. (MS), commonly known as Mallow, Malva or Khobiza (Arabic name), is native to North Africa, Europe and Asia. This annual herbaceous plant has a long

history of use as medicinal plant, as food and as animal feed. Stems, leaves and purple flowers are the apparent parts of Malva plant. Under favorable conditions, this plant can reach a height that exceeds 1.8 m.³² In this investigation, cellulosic fibers were extracted from the stems of MS plant using the ecological extraction technique.

Malva sylvestris L. stem anatomy

Plant anatomy is useful tool to study morphology, physiology and phylogeny of plant structure. Anatomical investigation was performed on a cross section of MS stem in the Biology department, University of M'sila, Algeria. The transversal stem section was made by using microtome. After that the thin section of Malva stem (350 μm) was prepared using double staining technique.^{33,34} Finally, the samples were placed on a microscope slide and examined using a Binocular Motic Microscope (BMM), this one is equipped with a camera and driving software Motic images 2000.

Fibers extraction

Malva sylvestris L. plant was collected in March 2020 from Maadhar (Bou-saada- Algeria). After harvesting, MS stems were separated from their leaves, roots and all impurities attached to them. A review of the literature shows that there are various techniques that can be used for the extraction of natural fibers from the plant.^{14,15,35-37} The commonly used extraction process are biological (retting or microbial degradation), mechanical and chemical one. Among these extraction methods, the biological technique is the most efficient method, and the easiest one, which produces high-quality of fiber.³⁸

The obtained stems were washed again with distilled water to ensure their cleanliness. After that, the stems were soaked into an usual container filled with tap water and covered for a period of 21 days (at room temperature) to undergo microbial degradation.^{14,21} As known, the water retting is a preferential rotting, which consume an amount of non cellulose compounds mainly waxes, pectin and hemicellulose.³⁹ After completion of retting, MS fibers were obtained by manual separation of fibers. Finally, MS fibers were washed several times with distilled water and then dried in oven at 70°C for 6 h. The extraction process of MS fibers from the plant to the fibers is shown in [Figure 2](#).

ATR-FTIR analysis

To determine the different chemical bonds and functional groups of MS fiber, Fourier transform infrared spectroscopy (ATR-FTIR) was used. A sample in powder form was placed on the ATR crystal and gently pushed out using a clip. Recordings were obtained using the Perkin-Elmer instrument with a spectral resolution of 4 cm^{-1} and wave number range of 4000-400 cm^{-1} .

X-ray diffraction spectroscopy

The XRD technology is used to find the crystal index (CI) of MS fibers. A fine powder sample was examined by the X'Pert-Pro SW diffraction scale with a reflection intensity of Cu K α radiation with a wavelength of ($\lambda = 1.54$) under a voltage of 40 kV and 30 mA (X-ray powder diffraction). The radiation reflection intensity was recorded for two values from 10° to 70° (angle range) with ambient temperature.

The crystal index (CI) of MS fibers was calculated using the following equation developed by Segal⁴⁰

$$CI\% = \left(\frac{I_{002} - I_{Am}}{I_{002}} \right) \times 100 \quad (1)$$

I_{002} is the maximum intensity (in arbitrary units) of crystalline phase, while, I_{am} is the intensity of amorphous.

Thermo-gravimetric analysis

Thermal stability of MS fiber was analyzed by thermo-gravimetric analysis using FANYUAN instrument DW5470H-3 STA. This analyze is one of the very important test that allows to know the limiting use of natural fibers, in term of thermal stability, as reinforcement in composite structures. An accurately weighed mass of MS powder (12.5 mg) was analyzed. The spectrum was recorded between the temperature range from 27°C and 600°C with a heating rate of 10°C/min.

In this study, the activation energy was obtained through Broido method

$$\ln \left[\ln \frac{1}{y} \right] = -\frac{E_a}{R} \left[\left(\frac{1}{T} \right) + K \right] \quad (2)$$

where y is normalized weight (w_t/w_o), w_t denotes the weight of the samples at any time t and w_o is the initial weight, E_a is the apparent activation energy, R is the universal gas constant (8.314 $\text{kJ}\cdot\text{mol}^{-1}$), while T is the absolute temperature in Kelvin and K is constant.

To prepare the ATG, XRD and ATR-FTIR samples, the fiber bundles were cut into small pieces, and then were dried (at 70°C during 1h), and were powdered into fine particle using Spex Mixer Mill.

Density measurement

The density of MS fibers was measured using a pycnometer for solid with volume of 50 mL according to ASTM D2320-9.⁴¹ The Density test was performed at laboratory condition (27°C and 50-60 RH). The arithmetic mean of five values was taken. Methanol with 0.791 g/cm^3 of density was used as immersion liquid. Before measurement, MS fibers were cut to 12-15 mm length, then they were dried at 60°C until the moisture content was reduced to below 5%.⁴² The apparent density ρ_{MS} is calculated using the relation

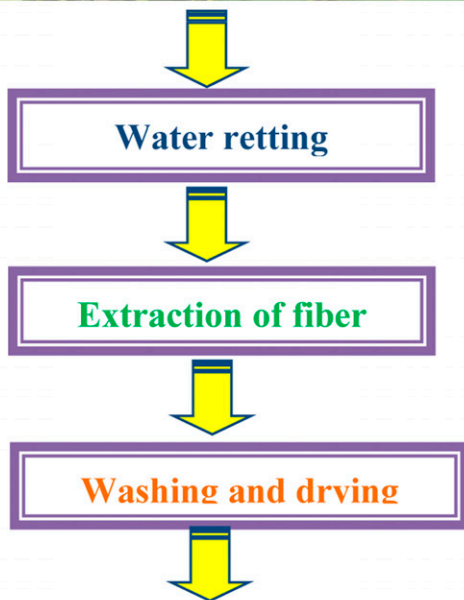


Figure 2. Extracted process of MS fibers.

$$\rho_{MS} = \frac{m_3 - m_1}{(m_2 - m_1) - (m_4 - m_3)} \rho_M \quad (3)$$

where: ρ_{MS} is the density of MS fiber (g/cm^3), ρ_M density of Methanol (g/cm^3)

m_1 : the mass of the empty pycnometer (g)

m_2 : mass of the pycnometer filled with Methanol (g)

m_3 : mass of the pycnometer filled with chopped MS fibers (g)

m_4 : mass of the pycnometer filled with chopped MS fibers and Methanol (g)

The cross-section area was calculated according to the relation⁴³

$$S_f = \frac{M}{\rho_{MS} \cdot L} \quad (4)$$

where S_f is the fiber cross section area, M is the fiber mass, L is the fiber length.

The fiber diameter was calculated from equation (4) by assuming a cylindrical shape by using the following formula:⁴⁴

$$D_{MS} = 2\sqrt{M/(\rho_{MS}\pi L)} \quad (5)$$

Where: D_{MS} is the diameter of the fiber, ρ_{MS} : the density of the fiber (g/cm^3), M : the mass of the fiber (g) and L : the length of the fiber (cm).

Fiber tensile testing

The mechanical properties of single fibers (Tensile strength, Young modulus and strain at failure) were determined from traction test as per standard test method for the tensile properties of single textile fibers (ASTM D3822-01),⁴⁵ as illustrated in Figure 3. The MS fibers were tested using Zwick Z100 with maximal capacity of 2.5 kN. The tests

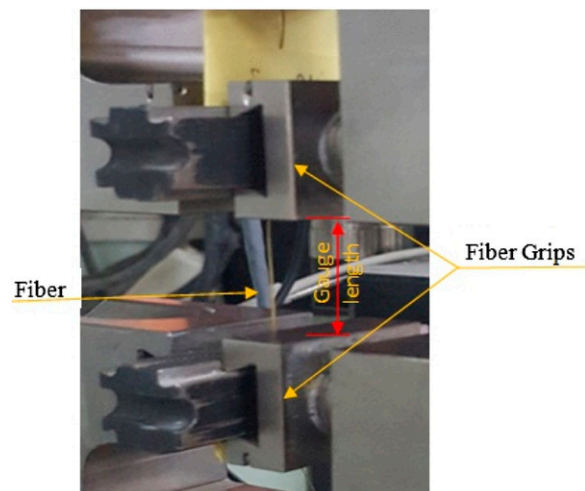


Figure 3. Setup of the tensile test of single fiber.

were carried out on specimens with 40 mm gage length using the displacement control at a rate of 2.5 mm/min. More than 30 fibers were tested to determine the average MS fiber properties.

Weibull distribution analysis

To predict the failure events of various data, Weibull method can be used.^{16,46–48} This method was popularized by Waloddi Weibull in 1951.⁴⁹ Recently, the Weibull analysis has been widely applied to the statistical analysis of mechanical properties of natural fiber.^{16,49,50}

The common two parameters Weibull distribution applied in this study are given by

$$F(\sigma) = 1 - \exp\left(-\frac{L}{L_0}\left(\frac{\sigma}{\sigma_0}\right)^m\right) \quad (6)$$

$$\ln\left(\ln\left(\frac{1}{1-F(\sigma)}\right)\right) - \ln\left(\frac{L}{L_0}\right) = m(\ln\sigma - \ln\sigma_0) \quad (7)$$

where $F(\sigma)$ is the failure probability of the fiber, L is the reference length, L_0 is the initial length. σ and σ_0 are respectively defined as the applied stress, and characteristic strength, and m is the Weibull modulus.

The parameters of the Weibull distribution were calculated through a linear regression analysis using the median rank value estimator which defined as follows

$$F(\sigma) = \frac{i - 0.3}{N + 0.4} \quad (8)$$

where N is the total number of samples and i the rank of the i th data point.

Morphology of fiber

To investigate the surface morphologies of MS fiber, a scanning electron microscopy, VEGA3 TESCAN was used (acceleration voltage are 15 and 20kV). Before the test, the studied fibers were coated with a thin gold film using a vacuum metallizer to render their surfaces conductive.

Results and discussion

Stem microscopy

In this investigation, the histological study is adopted to closely examine the anatomical structure of *Malva sylvestris* L. in order to check the presence of lignocellulosic fibers and their location in MS stem. Figure 4 shows the cross section of MS stem at different scales. As indicated, the stem of MS plant is organized in layers, and is built up from the outside to the inside respectively of epidermis, phloem, Xylem and the pith. The epidermis is external layer and is covered by a thin cuticle. Waxes and cuticle of the epidermis

covering the MS stem, and protect the plant. The phloem, or liber, conducts the developed sap, a solution of organic substances rich in carbohydrates, from the leaves to the other organs. The phloem consists mainly of cellulosic fibers, sieve tubes, and cellulosic parenchyma. The fibers are found in numerous groups and resemble those of the pericycle. The cambium is composed of one or more rows of meristematic cells. The xylem is much wider.^{21,51,52} The xylem conducts the raw sap, a liquid containing water and mineral salts drawn from the soil by the roots at the level of the piliferous layer, towards the leaves where photosynthesis takes place. The pith (medullary parenchyma) is rounded cells occupying the center of the stem with the presence of meatuses.

Density analysis

The major factor that distinguishes natural fibers from conventional ones is their low density. This lower density is more appropriate for lightweight application. In this investigation, the MS fiber was found to have a density of 1.12 ± 0.05 g/cm³. This value is very close to those of *Hyphaene thebaica* L.,¹⁴ *Dichrostachys Cinerea*,⁵³ *Arundo donax* L.,⁵⁴ *Acacia Arabica*,⁵⁵ *Cissus quadrangularis*,⁵⁶ *Cyperus pangorei*,⁵⁷ *Hierochloe Odarata*,⁵⁸ *Juncus effusus* L.³⁶ *Silybum marianum*.²⁴

ATR–FTIR analysis

The configuration information of the functional groups of MS fiber obtained by ATR–FTIR analysis is shown in the Figure 5. Hence, this result analysis shows that the infrared spectral bands share common absorption band with the majority of the studied lignocellulosic fibres. The large band observed between 3600–3000 cm^{−1} is associated with the hydrogen bonded O–H (Hydroxyl group) stretching vibration from the cellulose structure of MS.^{14,59} The absorption peaks at 2912 cm^{−1} and 2873 cm^{−1} are the characteristic of the C–H stretching vibration from CH and CH₂ group respectively.²³ Whilst the absorbance band located at 1733 cm^{−1} is a consequence of the stretching vibration of the (C = O) carbonyl groups of hemicellulose, lignin and extractives.^{19,22,60} The peak at 1625 cm^{−1} is attributed to the C = C stretching of the Alkenes groups of lignin.^{7,61} While a small peak at 1507 cm^{−1} indicates (C = C) stretching of the aromatic ring of the lignin compound.^{22,62,63} The absorbance band at 1421 cm^{−1} is associated to the CH₃ and CH₂ group symmetric bending from cellulose.^{19,36} The relatively weak bands at 1366 cm^{−1} and 1321 cm^{−1} are attributed to the bending vibration of C–H and C–O of the aromatic ring groups in the polysaccharides.⁵⁴ It should be noted that the band observed at 1237 cm^{−1} is due to the C–O–C stretching vibration for cellulose and hemicelluloses.⁶⁴

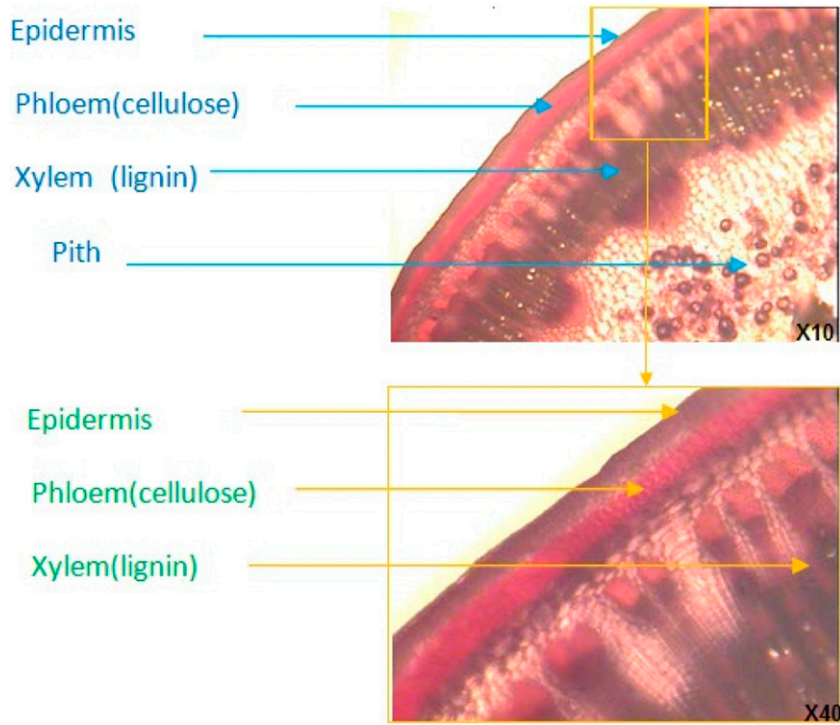


Figure 4. A cross section of a stem shows phloem (cellulosic fibers) and Xylem (lignified fibers) arranged in a ring around the periphery.

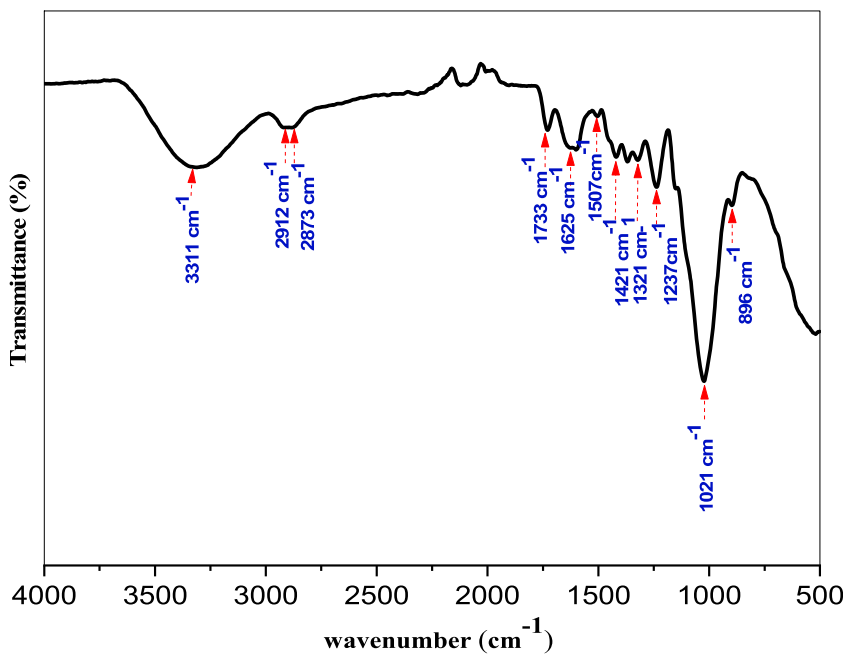


Figure 5. ATR- FTIR of MS fiber.

The sharp peak at 1021 cm^{-1} is associated to (C–O–C stretching of primary alcohol in cellulose and hemicellulose).¹⁹ In addition, the β -glycosidic linkage resulting from cellulose and hemicellulose in MS fiber was found around

896 cm^{-1} .^{14,65} The MS fibres which were tested in the present study and based on the analysis of the infrared spectral curve showed the presence of major components, which are (hemicellulose, cellulose and lignin). [Table 1](#)

Table 1. FTIR bands observed for MS fiber.

Bands position in this work Cm ⁻¹	Origin	References
3311	(Hydroxyl group) stretching vibration from the cellulose structure	14,59
2912–2873	C-H stretching vibration from CH and CH ₂ group respectively from cellulose and hemicellulose	19,55
1733	The stretching vibration of the (C = O) carbonyl groups of hemicellulose, lignin and extractives	19,53
1625	C = C stretching of the a Alkenes groups of lignin	7,61
1507	(C = C) stretching of aromatic ring of the lignin compound	62,63
1421	CH ₃ and CH ₂ group symmetric bending from cellulose	24,36
1321	C-H and C-O of the aromatic ring groups in the polysaccharides	54
1237	C–O–C stretching vibration for cellulose and hemicellulose	64
1021	(C–O–C stretching of primary alcohol in cellulose and hemicelluloses)	19
896	(C-O) groups which are related to the β-glycosidic linkages	16,65

summarizes the main ranges observed in the ATR–FTIR spectrum of MS fibers and the functional groups assigned to them.

X-ray diffraction analysis

The crystal index (CI) of cellulosic fiber is a crucial parameter because it directly influences greatly the mechanical properties. Based on the intensity method (empirical method of Segal, equation (1)), A Gaussian fitting protocol was used to determine peak position and intensity is illustrated in Figure 6, the MS fiber crystallinity index ($2\theta = 21^\circ.89$ corresponding to the cellulose I crystallographic plan 002 and $2\theta = 16^\circ.45$ corresponding to the amorphous fraction) was 55.12%, and when compared to other cellulosic fibers the (CI) of MS fibers was higher than that of the existing in *Lygeum Spartum* (46.19%), *Juncus effusus* (33.4%), *Acacia rabida* (51.72%), *Eleusineindica* (45%), *Ficus religiosa* (42.92%), *Prosopis juliflora* (46%), *ipomoea Staphylina* (43.96%).

Thermal analysis

Figure 7 illustrates the thermogravimetric (TGA) and its first derivative (DTG) curves of MS fiber. From this figure, the thermal decomposition consists of three stages of weight loss. Initially, the first stage corresponds to loss of absorbed moisture in MS fiber can be observed between 27°C and 110°C.¹⁴ The weight loss around this temperature was found to be 6.33 %. The second weight loss stage that ranged from 225°C to 355°C, which is related to the thermal decomposition of cellulosic substances (depolymerization of hemicellulose and cellulose). Reddy, et al.⁶⁶ indicated that a thermal degradation of a small fraction of lignin is also occurred in this stage. The change in shape of the DTG curve at temperature point 298°C seems to be

attributed to the decomposition of: (i) the main component of hemicellulose and (ii) the glycosidic linkages of cellulose. The weight loss in this temperature (298°C) was found to be about 33%. It is important to point out that a notable peak at 311°C, which is due to the maximum degradation rate of cellulose with the weight loss about 64 %. A possible depolymerization of lignin can also occur at this stage.⁶⁷ Finally, the thermal decomposition beyond 355°C–485°C characterizes the degradation of non-cellulosic materials such as lignin and pectin (third stage).^{8,14} In this stage, two small peaks are defined (at 383°C and 402°C). These ones may be linked to the thermal degradation of lignin and oxidative degradation of the charred residue.^{22,54} The weight loss at 485°C was found to be 83%. After that sample was completely calcined, and there are no outstanding features to report beyond.

Several authors have reported similar thermal degradation behavior to that described above when studying other natural fibers. On the other hand, various methods can be applied to TGA data to obtain kinetic parameters. Among these ones, the activation energy, E_a , is the most important factor that is very useful in reaching conclusions regarding the thermal stability of natural fibers, and can enhance its applicability in polymer composites for different applications.¹⁹ In other words, studying the thermal decomposition behavior can give a better understanding of the thermal stability of natural fibers for their subsequent use as a reinforcing element, especially in thermoplastic-matrix composites.⁸

The linear plot of $\ln [1/y]$ versus $1/T$ is shown in Figure 8. The activation energy value was obtained from the slope ($-E_a/R$). This one yielded activation energies of 111.29 kJ.mol⁻¹.

Generally, the range of activation energy for understanding fiber decomposition for polymer composite

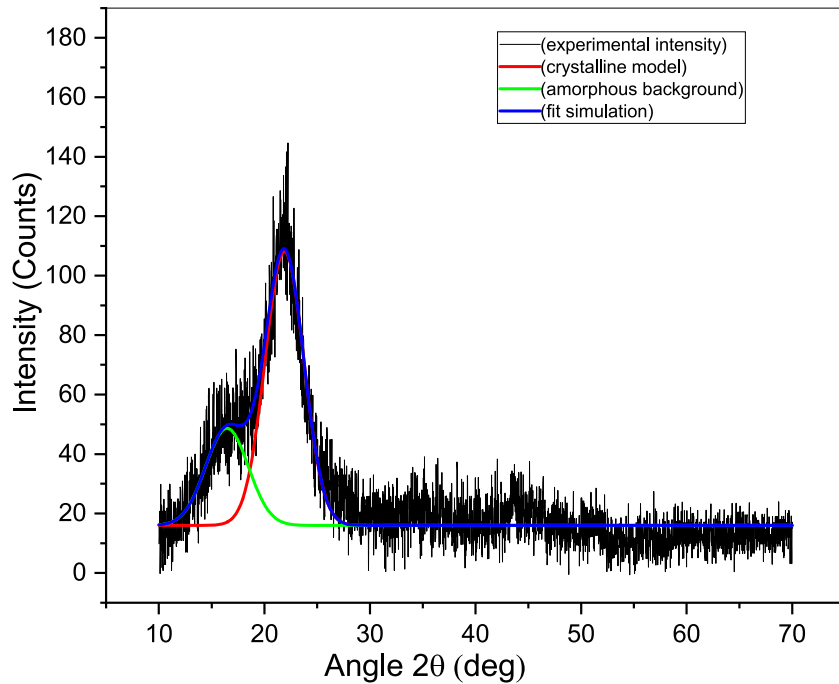


Figure 6. X-ray diffraction of MS fiber.

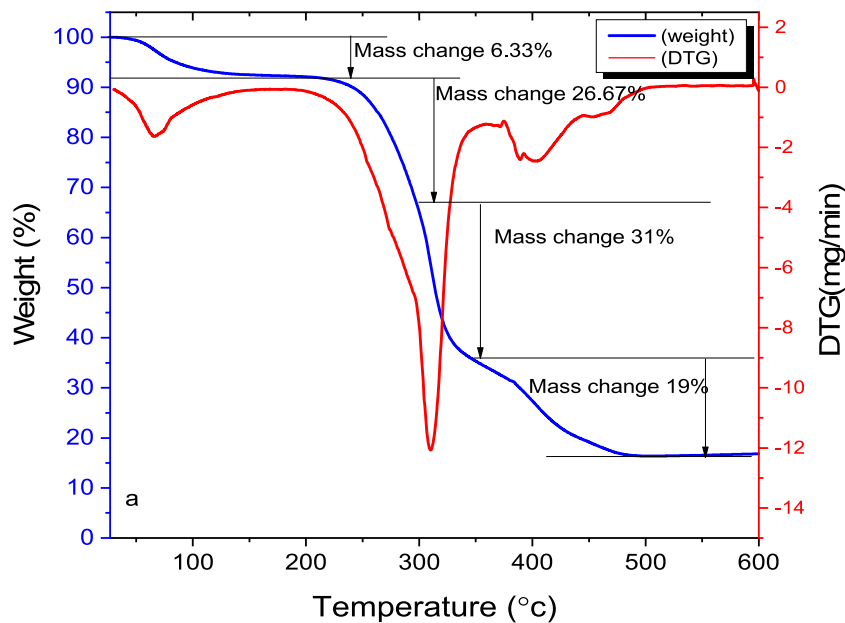


Figure 7. Thermogravimetric curve of MS fiber.

with respect to previously reported values is $60\text{--}170\text{ kJ}\cdot\text{mol}^{-1}$.⁶⁸ Table 2 summarizes the main thermal degradation characteristics of MS fiber, which are compared to other cellulosic fibers. The study of the thermal decomposition of MS fiber shows that it can be used as reinforcement in thermoplastic-matrix composites.

Tensile properties of MS fiber

The stress–strain response of MS fiber in traction loading is shown by Figure 9. This one illustrated typical behavior of this natural fiber when subjected in tensile loading. The relationship between stress and strain is quasi-linear up to fiber failure, which mentioned an elastic and brittle

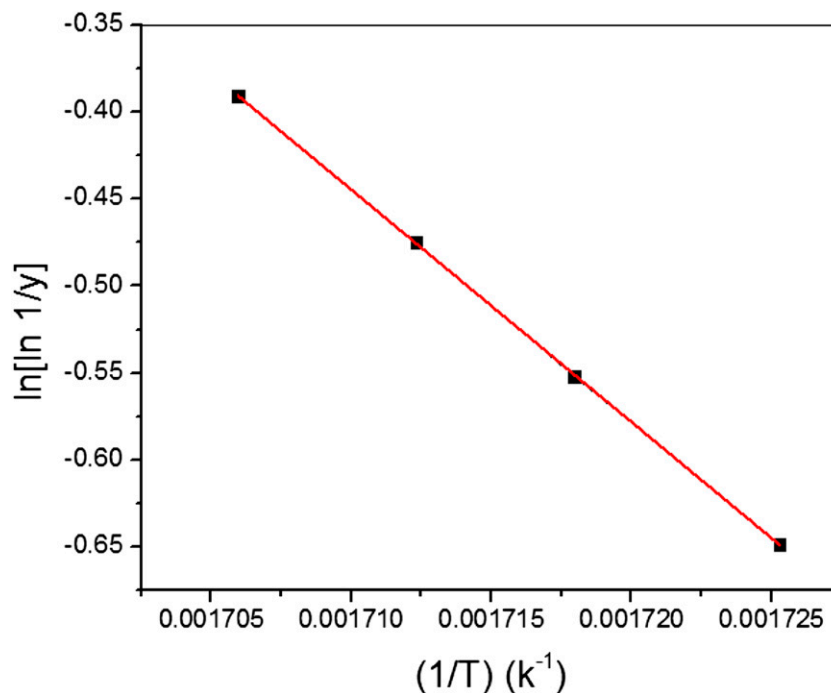


Figure 8. Broido's plot of MS fiber.

behavior. Similar evolution of stress–strain behavior was observed for *Coccinia grandis* L. *Juncus effusus* L. and *Arundo donax* L. which studied by Senthamarai Kannan and Kathiresan,⁶⁰ Maache, et al.³⁶ and Fiore, et al.⁵⁴ respectively.

The tensile test of MS fiber has allowed obtaining the main mechanical parameters including tensile strength, Young's modulus and strain at failure. The average arithmetic value and the standard deviation from the measurements are 236.64 ± 93.33 MPa, 26.07 ± 5.14 GPa, and $1.3 \pm 0.62\%$ respectively. As observed, the standard deviation was considerable. This is due to the lack of uniformity of fiber qualities, which are strongly depending on the location, time of harvest and processing conditions.⁶⁹

These properties were compared with other natural fibers from the published literatures and they are tabulated in Table 3. From this table, the MS fiber exhibited reasonable properties, which can be used in low cost applications.

Figure 10 shows the evolution of tensile strength and Young's modulus as a function of fiber diameter. As shown in this Figure, a decrease in tensile strength and Young's modulus is observed as the diameter of the fiber is increased. This dependency has already been reported by several authors.^{14,19,47,70} This decrease is partly explained by the calculating of the fiber diameter without taking into account the size of lumen which increases with the fiber diameter.^{47,70} The presence of non-cellulosic polysaccharides component rate,^{19,47} and/or the weaker or the damaged

micro-fibrils number with fiber diameter,¹⁴ can also lead to this dependency. On the other hand, the outside parameters (climate, age or maturity, soil quality, weather circumstances), extraction procedure and test parameters, can affect the scattering for one fiber to another.^{15,71} Therefore, it's necessary to use statistical approaches in order to evaluate its average tensile properties.

Statistical analysis

Logarithmic Weibull plots derived from MS fiber tensile tests are shown in Figure 11. As indicated, a good degree of linearity is observed (R^2 between 0.9444 and 0.999). In the case of natural fiber, the common values of Weibull modulus should be confined between 1 and 6.⁴⁶

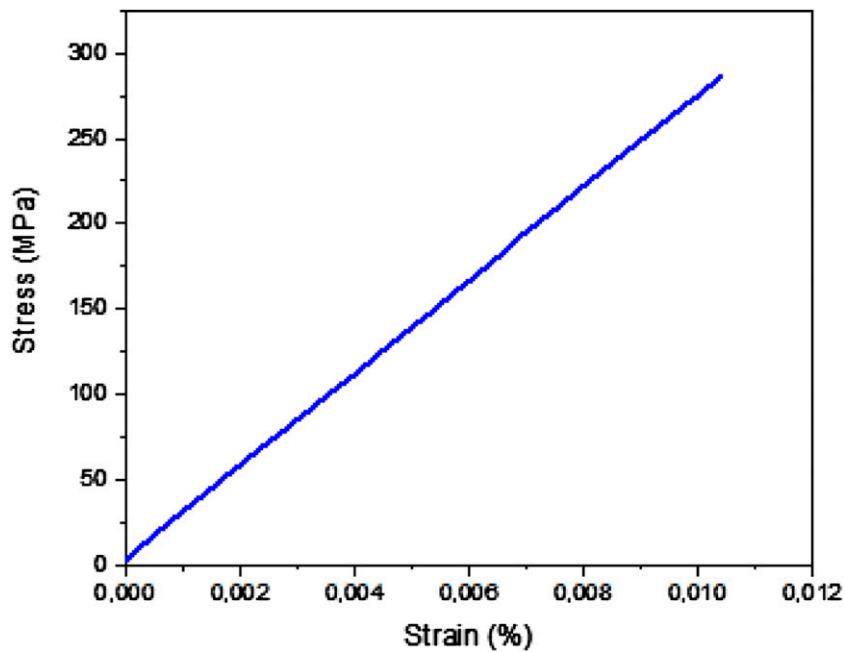
One can see that the Weibull modulus data in Table 4 are lying in the suggested range. The same Table represents the determined Weibull parameters which are compared with experimental ones. It's clear that the predicted tensile properties were observed to be in good agreement with the experimental results. Consequently, the Weibull function is able to effectively describe the statistical mechanical failure of lignocellulosic fibers.

SEM analysis

Figure 12 shows the morphologies of MS fiber. Transverse and longitudinal sections of the studied fiber

Table 2. Thermal analysis parameters of MS fiber in comparison with some other natural fibers.

Fiber	Max stability temperature T_s ($^{\circ}\text{C}$)	Max decomposition temperature T_d ($^{\circ}\text{C}$)	Activation energy E_a (kJ/mol)	References
Malva sylvestris L	225	311	111.29	Current work
Lygeum spartum	220	338.7	68.77	19
Arundo Donax L	275	320	—	54
Prosopis juliflora	217	331	76.7	22
Juncus effusus L.	220	360	—	36
Coccinia grandis.L	213.4	351.6	67.02	60
Calotropis gigantea	282	316	69.88	25
Cyperus pangorei	221	324	—	57
Dichrostachys Cinerea	226	359.3	—	53
Kigelia africana	212	340	—	65
Hyphaene thebaica L.	219	320	62.87	16

**Figure 9.** Typical tensile test curves for a single fiber.

were investigated. It can be observed in Figure 10(a) that the MS fiber is mainly formed by the fiber cells (elementary fiber or fibrils), and linked together by pectin and other non-cellulosic compounds (middle

lamella) to form the mechanically supporting structure.⁵⁴ These fiber cells are clearly visible when examining the transversal section of MS fiber (Figure 10(b)). In the center of each elementary fiber an

Table 3. Density and tensile properties of MS fibers and some natural fibers.

Plant species	Density (g/cm ³)	Diameter (μm)	Tensile strength (MPa)	Young's modulus (GPa)	Strain at break (%)	Ref
Malva sylvestris	1.12 ± 0.05	149.03 ± 73.11	236.64 ± 113	26.07 ± 8.6	1.3 ± 0.6	Current work
Juncus effusus L	1.139	280 ± 56	113 ± 36	4.38 ± 1.37	2.75 ± 0.6	36
Lygeum Spartum L	1.4997 ± 0.003	180–433	64.63–280.03	4.47–13.27	1.49–3.74	19
Arundo Donax L	1; 168	—	248	9.4	3.24	54
Ficus religiosa	1.246	25.63	433.32 ± 44	5.42 ± 2.6	8.74 ± 1.8	29
Coccinia Grandis L	1.243 ± 0.0226	27.33 ± 0.3789	273 ± 27.74	10.17 ± 1.261	2.703 ± 0.27	60
Hyphaene Thebaica L.	1.19 ± 0.05	137.02–220.42	124.84–448.10	8.06–19.59	0.81–2.86	16
Hierochloe Odarata	1.16 ± 0.02	136.71 ± 4.34	105.73 ± 35.42	2.56 ± 0.98	2.37 ± 0.95	58
Cissus Quadrangularis	1.22	—	4203 ± 1276	131 ± 37	4.78 ± 1; 24	27
Cyperus Pangorei	1.102	133.1 ± 17	196 ± 56	11; 6 ± 2.61	1.69	57
Silybum Marianum	1.098	222	201.16	15.97	1.593	24
Dichrostachys Cinerea	1.24	—	873 ± 14	—	—	53
Acacia Arabica	1.028	—	—	—	—	55

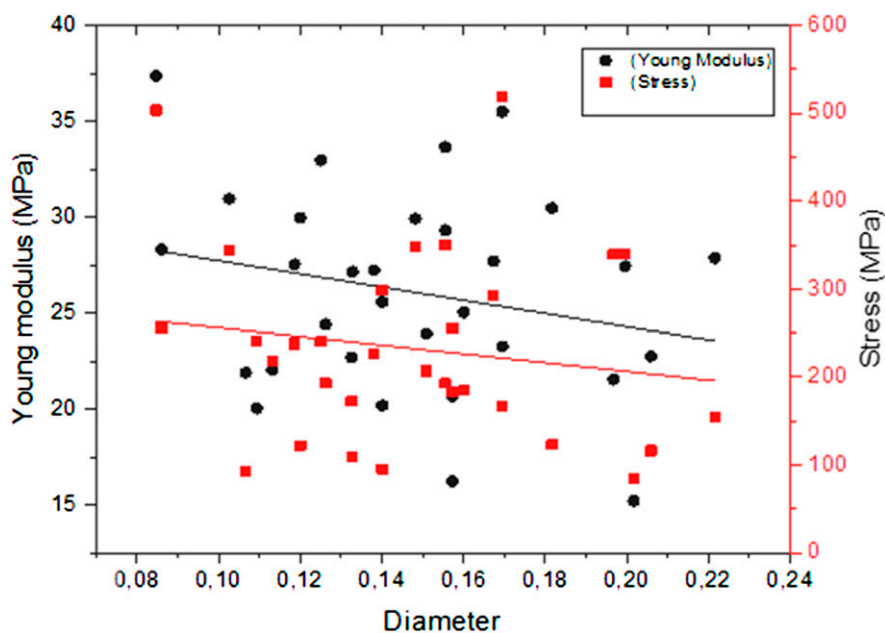


Figure 10. Stress at break and Young's modulus as a function of fiber diameter.

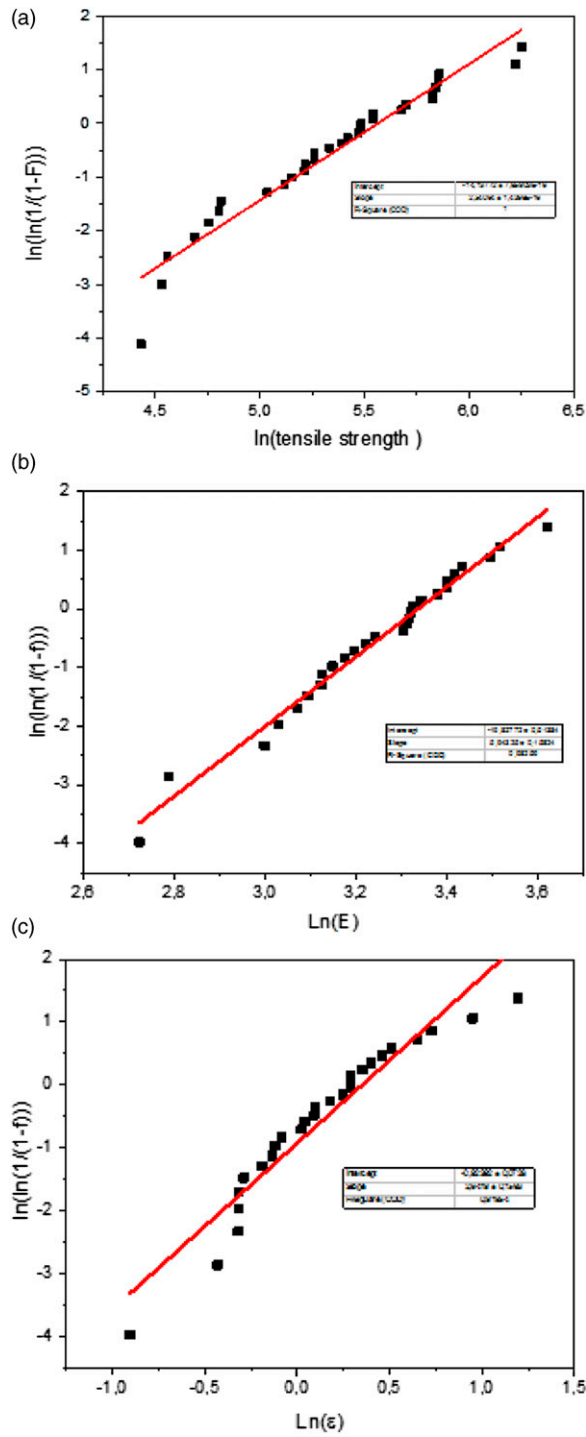
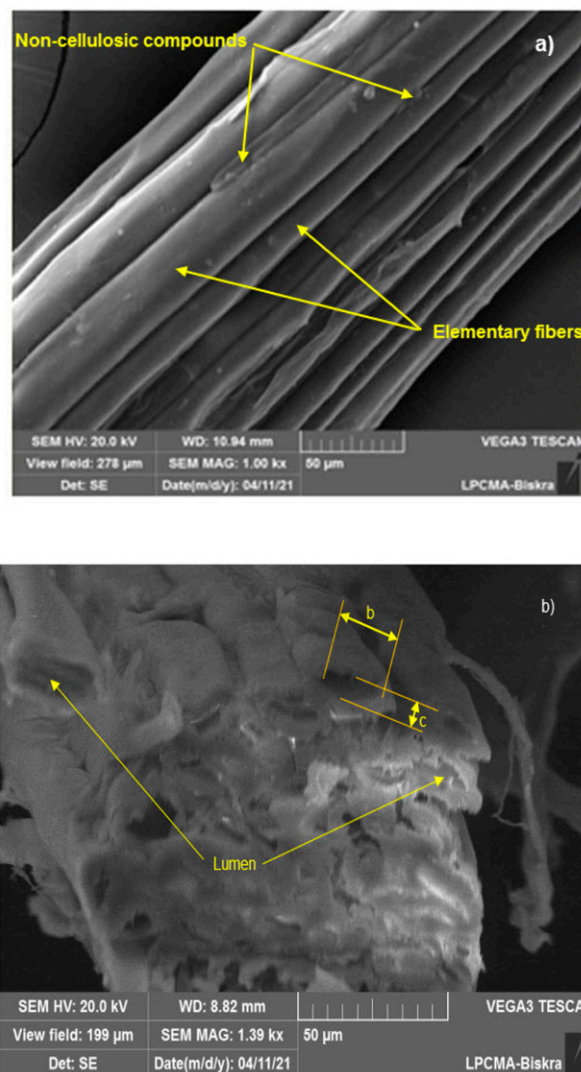


Figure 11. Weibull plot of MS fiber mechanical failure and fitted Weibull reliability distribution for (a) tensile strength, (b) Young's modulus, and (c) Strain at failure.

Table 4. Mechanical characteristics of MS fibers obtained by Weibull distribution.

Plant species	Tensile strength (MPa)			Young's modulus (GPa)			Strain at failure (μm)		
	Weibull		exp	Weibull		exp	Weibull		exp
	m	σ_0	σ	m	E_0	E	m	ε_0	ε
<i>Malva sylvestris</i>	3.02	267.57	236.64	5.94	28.12	26.07	2.4	1.41	1.3

**Figure 12.** SEM micrographs of MS fiber: a) longitudinal view, b) transverse section view.

empty space, called lumen, is observed. This one has an elliptical or slightly oval shape ($a = 4 \mu\text{m}$ and $b = 15 \mu\text{m}$), which is responsible for transporting water and nutrients along the fiber.³ The thickness of the cell wall is around $6 \mu\text{m}$ approximately.

Conclusion

In this experimental study, lignocellulosic fibers extracted from *Malva sylvestris* L. were characterized. The morphological, physico-chemical, thermal, and mechanical

characteristics of MS fiber were determined. The main conclusions which can be drawn are the following:

- Microstructural analysis of MS fibers shows that MS bark is reached on fiber cells connected with non-cellulosic components.
- MS fibers are characterized by low unit weight which helps to use it as reinforcements for composites in order to produce lightweight material.
- The tensile properties obtained from single fiber tests show values are 236.64 ± 93.33 MPa for tensile strength and 26.07 ± 5.14 GPa for Young modulus.
- Statistical analysis showed a good agreement between the Weibull distribution parameters and the experimental results.
- Crystallinity index for MS fibers is about of 55.12%, which indicates a high cellulose content.
- MS fibers are thermally stable until 225°C and characterized by an activation energy of about 111 kJ.mol⁻¹.

Declaration of conflicting interests

The author(s) declared no potential conflicts of interest with respect to the research, authorship, and/or publication of this article.

Funding

The author(s) received no financial support for the research, authorship, and/or publication of this article.

ORCID iD

Mansour Rokbi  <https://orcid.org/0000-0001-5856-662X>

References

1. Mansour R, El Abidine RZ and Brahim B. Performance of polymer concrete incorporating waste marble and alfa fibers. *Adv Con Construc* 2017; 5: 331–343.
2. Sudhakar U, Suresh B and Bahubalendruni MR. A review on physical and chemical properties of natural fiber reinforced composite materials. *Int J Sci Dev Res* 2018; 3: 160–172.
3. Sanjay M, Madhu P, Jawaid M, et al. Characterization and properties of natural fiber polymer composites: a comprehensive review. *J Clean Prod* 2018; 172: 566–581.
4. Ponnu Krishnan P and Rajadurai SJ. Microscopical, physico-chemical, mineralogical, and mechanical characterization of Sansevieria zeylanica fibers as potential reinforcement of composite structures. *J Compos Mater* 2017; 51: 811–829.
5. Noureddine M. Study of composite-based natural fibers and renewable polymers, using bacteria to ameliorate the fiber/matrix interface. *J Compos Mater* 2019; 53: 455–461.
6. Huda M, Drzal L, Ray D, et al. Natural-fiber composites in the automotive sector. In: *Properties and performance of natural-fibre composites*, 2008, pp. 221–268.
7. Ahmed J, Balaji M, Saravanakumar S, et al. A comprehensive physical, chemical and morphological characterization of novel cellulosic fiber extracted from the stem of Elettaria cardamomum plant. *J Nat Fibers* 2021; 18: 1460–1471.
8. Hossain MK, Dewan MW, Hosur M, et al. Effect of surface treatment and nanoclay on thermal and mechanical performances of jute fabric/biopol ‘green’ composites. *J Reinfor Plast Comp* 2011; 30: 1841–1856.
9. Koppiahraj K, Bathrinath S, Narayanasamy P, et al. A review on the factors influencing natural fiber composite materials. *Hybrid Nat Fiber Compo* 2021; 13: 185–205.
10. Sikame Tagne N, Abessolo D, Harzallah O, et al. Physico-chemical and mechanical characterization of bambusa vulgaris fibers from Cameroon. *J Compos Mater* 2021; 55: 2489–2502.
11. Kadumudi FB, Trifol J, Jahanshahi M, et al. Flexible and green electronics manufactured by origami folding of nanosilicate-reinforced cellulose paper. *ACS Appl Mater Inter* 2020; 12: 48027–48039.
12. Mehrali M, Bagherifard S, Akbari M, et al. Blending electronics with the human body: a pathway toward a cybernetic future. *Adv Sci* 2018; 5: 1700931.
13. Gallos A, Paës G, Allais F, et al. Lignocellulosic fibers: a critical review of the extrusion process for enhancement of the properties of natural fiber composites. *RSC Adv* 2017; 7: 34638–34654.
14. Mansour R, Abdelaziz A and Fatima Zohra A. Characterization of long lignocellulosic fibers extracted from Hyphaene thebaica L. leaves. *Res J Textile Apparel* 2018; 22: 195–211.
15. Bezazi A, Belaadi A, Bourchak M, et al. Novel extraction techniques, chemical and mechanical characterisation of Agave americana L. natural fibres. *Compo Part B: Eng* 2014; 66: 194–203.
16. Lemita N, Deghboudj S, Rokbi M, et al. Characterization and analysis of novel natural cellulosic fiber extracted from Strelitzia reginae plant. *J Compos Mater* 2022; 56: 99–114.
17. AliAkbari R, Ghasemi MH, Neekzad N, et al. High value add bio-based low-carbon materials: conversion processes and circular economy. *J Clean Prod* 2021; 293: 126101.
18. Marques G, Rencoret J, Gutiérrez A, et al. Evaluation of the chemical composition of different non-woody plant fibers used for pulp and paper manufacturing. *The Open Agric J* 2010; 4: 93–101.
19. Belouadah Z, Ati A and Rokbi M. Characterization of new natural cellulosic fiber from Lygeum spartum L. *Carbohydr Poly* 2015; 134: 429–437.
20. Ahmed MJ, Balaji M, Saravanakumar S, et al. A comprehensive physical, chemical and morphological characterization of novel cellulosic fiber extracted from the stem of Elettaria cardamomum plant. *J Nat Fibers* 2019; 18: 1–12.
21. Kılınç AÇ, Köktaş S, Atagür M, et al. Effect of extraction methods on the properties of althea officinalis L. fibers. *J Nat Fibers* 2018; 15: 325–336.

22. Saravanakumar S, Kumaravel A, Nagarajan T, et al. Characterization of a novel natural cellulosic fiber from *Prosopis juliflora* bark. *Carbohydr Polymers* 2013; 92: 1928–1933.
23. Moussaoui N, Rokbi M, Osmani H, et al. Extraction and characterization of fiber treatment *Inula viscosa* fibers as potential polymer composite reinforcement. *J Polym Environ* 2021; 29: 3779–3793.
24. Laifa F, Rokbi M, Amroune S, et al. Investigation of mechanical, physicochemical, and thermal properties of new fiber from *Silybum marianum* bark fiber. *J Compos Mater* 2022; 56: 00219983221090020–00219983221092238.
25. Narayanasamy P, Balasundar P, Senthil S, et al. Characterization of a novel natural cellulosic fiber from *Calotropis gigantea* fruit bunch for ecofriendly polymer composites. *Int Journal Biological Macromole* 2020; 150: 793–801.
26. Gurukarthik Babu B, Prince Winston D, SenthamaraiKannan P, et al. Study on characterization and physicochemical properties of new natural fiber from *Phaseolus vulgaris*. *J Nat Fibers* 2019; 16: 1035–1042.
27. Indran S, Raj RE and Sreenivasan V. Characterization of new natural cellulosic fiber from *Cissus quadrangularis* root. *Carbohydr Polymers* 2014; 110: 423–429.
28. Ganapathy T, Sathiskumar R, SenthamaraiKannan P, et al. Characterization of raw and alkali treated new natural cellulosic fibres extracted from the aerial roots of banyan tree. *Int J Biolo Macromole* 2019; 138: 573–581.
29. Moshi AAM, Ravindran D, Bharathi SS, et al. Characterization of a new cellulosic natural fiber extracted from the root of *Ficus religiosa* tree. *Int J Biological Macromole* 2020; 142: 212–221.
30. Bhatnagar A and Sain M. Processing of cellulose nanofiber-reinforced composites. *J Reinforced Plastics Composites* 2005; 24: 1259–1268.
31. Hepworth D, Hobson R, Bruce D, et al. The use of unretted hemp fibre in composite manufacture. *Compo Part A: Appl Sci Manufac* 2000; 31: 1279–1283.
32. Mousavi SM, Hashemi SA, Behbudi G, et al. A review on health benefits of *Malva sylvestris* L. nutritional compounds for metabolites, antioxidants, and anti-inflammatory, anticancer, and antimicrobial applications. *Evidence-Based Complementary and Alternative Medicine*, 2021.
33. Peršin Z, Maver U, Pivec T, et al. Novel cellulose based materials for safe and efficient wound treatment. *Carbohydr Polymers* 2014; 100: 55–64.
34. Silva CJD, Lima LHFd, Paiva PMd, et al. An inexpensive and environmentally friendly staining method for semi-permanent slides from plant material probed using anatomical and computational chemistry analyses. *Rodriguésia* 2020; 71: 1–20.
35. Paixão WA, Martins LS, Zanini NC, et al. Modification and characterization of cellulose fibers from palm coated by $ZrO_2 \cdot nH_2O$ particles for sorption of dichromate ions. *J Inorg Organomet Polym Mater* 2020; 30: 2591–2597.
36. Maache M, Bezazi A, Amroune S, et al. Characterization of a novel natural cellulosic fiber from *Juncus effusus* L. *Carbohydr Polymers* 2017; 171: 163–172.
37. Zanini N, Carneiro E, Menezes L, et al. Palm fibers residues from agro-industries as reinforcement in biopolymer filaments for 3D-printed scaffolds. *Fibers Polym* 2021; 22: 2689–2699.
38. Zhang L, Zhu R, Chen J, et al. Seawater-retting treatment of hemp and characterization of bacterial strains involved in the retting process. *Process Biochem* 2008; 43: 1195–1201.
39. Banik S, Basak M, Paul D, et al. Ribbon retting of jute—a prospective and eco-friendly method for improvement of fibre quality. *Ind Crops Prod* 2003; 17: 183–190.
40. Segal L, Creely JJ, Martin A Jr., et al. An empirical method for estimating the degree of crystallinity of native cellulose using the X-ray diffractometer. *Textile Res J* 1959; 29: 786–794.
41. ASTM D2320-9. Standard test method for density (relative density) of solid pitch (Pycnometer Method), 2017.
42. Amel BA, Paridah MT, Sudin R, et al. Effect of fiber extraction methods on some properties of kenaf bast fiber. *Ind Crops Prod* 2013; 46: 117–123.
43. Brahim SB and Cheikh RB. Influence of fibre orientation and volume fraction on the tensile properties of unidirectional Alfa-polyester composite. *Composites Sci Technology* 2007; 67: 140–147.
44. Msahli S, Ydrean J and Sakli F. Evaluating the fineness of agave americana L. fibers. *Textile Res J* 2005; 75: 540–543.
45. ASTM D3822-01. Standard Test Method for Tensile Properties of Single Textile Fibers1: ASTM International, 2007.
46. Ibrahim I, Sarip S, Bani N, et al. The Weibull probabilities analysis on the single kenaf fiber. In: AIP Conference Proceedings, 2018, 1958:020009. AIP Publishing LLC.
47. Duval A, Bourmaud A, Augier L, et al. Influence of the sampling area of the stem on the mechanical properties of hemp fibers. *Mater Letters* 2011; 65: 797–800.
48. Naik DL and Fronk TH. Weibull distribution analysis of the tensile strength of the kenaf bast fiber. *Fibers Polym* 2016; 17: 1696–1701.
49. Cheung H-Y, Lau K-T, Ho M-P, et al. Study on the mechanical properties of different silkworm silk fibers. *J Compos Mater* 2009; 43: 2521–2531.
50. Sia CV, Nakai Y, Shiozawa D, et al. Statistical analysis of the tensile strength of treated oil palm fiber by utilisation of Weibull distribution model. *Open J Compos Mater* 2014; 2014: 72–77.
51. Shaltout K. Dimension analysis of *Thymelaea hirsuta* (L.) Endl. fibers. *Feddes Repertorium* 1992; 103: 99–106.
52. Kabeya KP, Robbertse PJ, Marais D, et al. Plant anatomy as a tool for evaluating the effect of different levels of nitrogen, plant population density, row spacing and irrigation on kenaf (*Hibiscus cannabinus*) fibre development. *South Afr J Plant Soil* 2017; 34: 351–360.

53. Baskaran P, Kathiresan M, Sentharamaikannan P, et al. Characterization of new natural cellulosic fiber from the bark of *dichrostachys cinerea*. *J Nat Fibers* 2018; 15: 62–68.
54. Fiore V, Scalici T and Valenza A. Characterization of a new natural fiber from *Arundo donax* L. as potential reinforcement of polymer composites. *Carbohydr Polymers* 2014; 106: 77–83.
55. Manimaran P, Saravanakumar S, Mithun N, et al. Physico-chemical properties of new cellulosic fibers from the bark of *Acacia arabica*. *Int J Polym Anal Characterization* 2016; 21: 548–553.
56. Indran S and Raj RE. Characterization of new natural cellulosic fiber from *Cissus quadrangularis* stem. *Carbohydr Polymers* 2015; 117: 392–399.
57. Mayandi K, Rajini N, Pitchipoo P, et al. Extraction and characterization of new natural lignocellulosic fiber *Cyperus pangorei*. *Int J Polym Anal Characterization* 2016; 21: 175–183.
58. Dalmis R, Köktaş S, Seki Y, et al. Characterization of a new natural cellulose based fiber from *Hierochloe Odarata*. *Cellulose* 2020; 27: 127–139.
59. Chikouche MDL, Merrouche A, Azizi A, et al. Influence of alkali treatment on the mechanical properties of new cane fibre/polyester composites. *J Reinforced Plastics Composites* 2015; 34: 1329–1339.
60. Sentharamaikannan P and Kathiresan M. Characterization of raw and alkali treated new natural cellulosic fiber from *Coccinia grandis*. L. *Carbohydr Polymers* 2018; 186: 332–343.
61. Khan A, Vijay R, Singaravelu DL, et al. Extraction and characterization of natural fiber from *Eleusine indica* grass as reinforcement of sustainable fiber reinforced polymer composites. *J Nat Fibers* 2021; 18: 1742–1750.
62. Jayaramudu J, Guduri B and Rajulu AV. Characterization of new natural cellulosic fabric *Grewia tilifolia*. *Carbohydr Polymers* 2010; 79: 847–851.
63. Sarikanat M, Seki Y, Sever K, et al. Determination of properties of *Althaea officinalis* L. (Marshmallow) fibres as a potential plant fibre in polymeric composite materials. *Composites Part B: Eng* 2014; 57: 180–186.
64. Jabbar A, Militký J, Wiener J, et al. Tensile, surface and thermal characterization of jute fibres after novel treatments. *Indian J Fibre Text Res* 2016; 41: 249–254.
65. Siva R, Valarmathi T, Palanikumar K, et al. Study on a Novel natural cellulosic fiber from *Kigelia africana* fruit: characterization and analysis. *Carbohydr Polymers* 2020; 244: 116–494.
66. Reddy KO, Maheswari CU, Dhlamini M, et al. Extraction and characterization of cellulose single fibers from native african napier grass. *Carbohydr Polymers* 2018; 188: 85–91.
67. Reddy KO, Ashok B, Narender Reddy KR, et al. Extraction and characterization of novel lignocellulosic fibers from *Thespesia lampas* plant. *Int J Polym Anal Characterization* 2014; 19: 48–61.
68. Yao F, Wu Q, Lei Y, et al. Thermal decomposition kinetics of natural fibers: activation energy with dynamic thermogravimetric analysis. *Polym Degrad Stab* 2008; 93: 90–98.
69. Faruk O, Bledzki AK, Fink HP, et al. Progress report on natural fiber reinforced composites. *Macromolecular Mater Eng* 2014; 299: 9–26.
70. Pillin I, Kervoelen A, Bourmaud A, et al. Could oleaginous flax fibers be used as reinforcement for polymers? *Ind Crops Prod* 2011; 34: 1556–1563.
71. Santhanam K, Kumaravel A, Saravanakumar S, et al. Characterization of new natural cellulosic fiber from the *Ipomoea staphylina* plant. *Int J Polym Anal Characterization* 2016; 21: 267–274.